J. Fluid Mech. (1976), *vol.* 75, *part* 1, *pp.* 17–28
Printed in Great Britain

The low frequency sound from multipole sources in axisymmetric shear flows. Part 2

By M. E. GOLDSTEIN

National Aeronautics and Space Administration, Lewis Research Center, Cleveland, Ohio 44135

(Received 1 July 1975)

A previous analysis of the acoustic radiation from multipole sources is extended to include additional components of the dipole and quadrupole sources. It is found that, unlike the components of the sources considered in the previous paper, the exponent of the Doppler factor now depends on the location of the sources within the jet.

1. Introduction

In an earlier paper by Goldstein (1975; hereafter referred to as I) closed-form solutions were obtained for the acoustic radiation from certain types of multipole sources imbedded in an infinite cylindrical jet (see figure 1 of I). The results are valid in the limit where the wavelength of the sound is long compared with the jet radius. The types of sources considered were monopoles, dipoles with their axes aligned with the flow direction (Z direction), and r–Z, θ–Z and Z–Z quadrupoles. But of these three quadrupole sources, only the r–Z component was found to contribute to the low frequency sound field. It was shown that the exponent n of the Doppler factor $(1-M\cos\theta)^{-n}$ multiplying the pressure signal from this quadrupole was increased by the mean flow, thus providing a possible explanation for the observed concentration of low frequency sound on the downstream axes of real air jets. However, the results raised the question of whether or not the components of the quadrupole which were not considered could also contribute appreciably to the on-axis sound. In the present paper we attempt to answer this question by considering the remaining components of the dipole and quadrupole sources. All these components are found to contribute to the radiation field but, unlike the sources considered in I, the resulting formulae for the acoustic pressure no longer depend only on the local properties of the flow. Instead they exhibit a dependence on the complete velocity profile.

The general formulae for the acoustic radiation are expressed in terms of a certain homogeneous solution to an ordinary differential equation. This solution is worked out in detail for a jet with a power-law velocity profile (i.e. $U \sim 1-r^{\lambda}$, where λ can be any positive number) and specific formulae for the radiation field are given for this case. Approximate formulae, which are very easy to interpret physically, are also given. They show that the exponents of the Doppler factors of the quadrupole sources considered in this paper are, in the main, not changed

as much by the mean flow as those of the quadrupole sources considered in I. Moreover these exponents are now found to depend on both the position of the sources in the jet and the shape of the mean velocity profile. In most cases the sources exhibit a behaviour which is intermediate between that of the sources studied in I and that of sources moving through a stationary medium.

2. Analysis

The notation used in this paper is the same as that used in I. In the latter report it was shown that for dipole and higher-order sources the τ–Z Fourier-transformed pressure

$$P(r,\phi|k,\epsilon) = \frac{1}{(2\pi)^2}\int_{-\infty}^{\infty}\int_{-\infty}^{\infty} \exp\left[i(\epsilon\tau + kZ)\right] p\, d\tau\, dZ \tag{1}$$

is governed by the equation

$$\nabla_t^2 P - \frac{2\kappa U'}{1+\kappa U}\frac{\partial P}{\partial r} + \epsilon^2[M^2(1+\kappa U)^2 - \kappa^2]\, P$$
$$= \frac{r_0(1+\kappa U)^2}{(2\pi)^2}\int_{-\infty}^{\infty}\int_{-\infty}^{\infty} \exp\left[i\epsilon(\kappa Z+\tau)\right]\nabla.\left[\frac{\mathbf{f}}{(\kappa+\kappa U)^2}\right] dZ\, d\tau. \tag{2}$$

We obtained a solution to this equation which is valid for small values of the dimensionless frequency $\epsilon = \omega r_0/U_s$ (with $\kappa = k/\epsilon$ of order one) but considered only the case where the volume force (dipole strength) $\mathbf{f}$ is purely axial (i.e. $\mathbf{f} = \hat{\mathbf{k}}_3 f_3$, where $\hat{\mathbf{k}}_3$ is a unit vector in the direction of the mean flow). In the present report we shall consider the remaining transverse component $\mathbf{f}_t \equiv \mathbf{f} - \hat{\mathbf{k}}_3 f_3$ of this force. Then, in the region near the jet where r is of order one (i.e. the inner region) we seek an expansion of the form

$$P = \epsilon \ln \epsilon P^{(-1)} + P^{(0)} + \alpha(\epsilon)\, P^{(1)} \ldots, \quad \alpha(\epsilon) = O(\epsilon),$$

and obtain in the limit as $\epsilon \to 0$ with r held fixed

$$\nabla_t^2 P^{(-1)} - \frac{2\kappa U'}{1+\kappa U}\frac{\partial P^{(-1)}}{\partial r} = 0,$$

$$\nabla_t^2 P^{(0)} - \frac{2\kappa}{1+\kappa U}U'\frac{\partial P^{(0)}}{\partial r} = \frac{r_0(1+\kappa U)^2}{(2\pi)^2}\nabla.\int_{-\infty}^{\infty}\int_{-\infty}^{\infty}$$
$$\times \exp\left[i\epsilon(\kappa Z+\tau)\right]\left[\frac{\mathbf{f}_t}{(1+\kappa U)^2}\right] dZ\, d\tau.$$

If we now expand the solution to the latter equation in the Fourier series

$$P^{(0)} = \sum_{n=-\infty}^{\infty} P_n^{(0)}(r)\, e^{in\phi}$$

we find that the lowest-order Fourier coefficients are determined by

$$\frac{d}{dr}\left[\frac{r}{(1+\kappa U)^2}\frac{dP_0^{(0)}}{dr}\right] = \frac{rr_0}{(2\pi)^3}\int_0^{2\pi}\int_{-\infty}^{\infty}\int_{-\infty}^{\infty} \nabla.\exp\left[i\epsilon(\kappa Z+\tau)\right]\left[\frac{\mathbf{f}_t}{(1+\kappa U)^2}\right] dZ\, d\tau\, d\phi \tag{3}$$

and

$$\frac{(1+\kappa U)^2}{r}\frac{d}{dr}\left(\frac{r}{(1+\kappa U)^2}\frac{dP_{\pm1}^{(0)}}{dr}\right)-\frac{1}{r^2}P_{\pm1}^{(0)}$$
$$=\frac{(1+\kappa U)^2 r_0}{(2\pi)^3}\int_0^{2\pi}\int_{-\infty}^{\infty}\int_{-\infty}^{\infty}\exp\left[i\epsilon(\kappa Z+\tau)\mp i\phi\right]\nabla.\left[\frac{\mathbf{f}_t}{(1+\kappa U)^2}\right]dZ\,d\tau\,d\phi. \quad (4)$$

But integrating (3) twice shows that

$$P_0^{(0)}=\text{constant}+\frac{r_0}{(2\pi)^3}\int_0^r\frac{(1+\kappa U)^2}{r}$$
$$\times\left\{\int_0^r\int_0^{2\pi}\int_{-\infty}^{\infty}\int_{-\infty}^{\infty}\nabla.\exp\left[i\epsilon(\kappa Z+\tau)\right]\left[\frac{\mathbf{f}_t}{(1+\kappa U)^2}\right]r\,dr\,d\phi\,dZ\,d\tau\right\}dr.$$

Consequently, assuming that $\mathbf{f}_t$ vanishes faster than any power of r as $r\to\infty$, we find that as $r\to\infty$

$$P_0^{(0)}\sim b_0+c_0\ln r+\text{terms which are smaller than any power of } r,$$

where c_0 is given by

$$c_0=\frac{r_0}{(2\pi)^3}\int_{-\infty}^{\infty}\int\nabla.\exp\left[i\epsilon(\kappa Z+\tau)\right]\left[\frac{\mathbf{f}_t}{(1+\kappa U)^2}\right]d\mathbf{y}\,d\tau;$$

the omission of the limits on the second integral indicates that the integration is to be carried out over all space and $d\mathbf{y}$ denotes a three-dimensional volume element. But applying the divergence theorem shows that $c_0=0$. Hence, as $r\to\infty$

$$P_0^{(0)}\sim b_0+\text{arbitrarily small terms.} \quad (5)$$

On the other hand, the results in appendix A show that, if the source distribution decays sufficiently rapidly,

$$P_1^{(0)}\sim c_1^{\pm}r^{\pm1},\quad P_{-1}^{(0)}\sim c_{-1}^{\pm}r^{\pm1}\quad\text{as}\quad r\to\infty,$$

where
$$c_{\pm1}^{-}=\frac{r_0}{(2\pi)^3}\int_{-\infty}^{\infty}\int\frac{\exp\left[i\epsilon(\kappa Z+\tau)\right]}{(1+\kappa U)^2}\mathbf{f}_t.\nabla\left[\frac{Y_1(\kappa,r)}{2Y_1'(\kappa,\infty)}e^{\mp i\phi}\right]d\mathbf{y}\,d\tau \quad (6)$$

and $Y_1(\kappa,r)$ is any homogeneous solution of (4) which vanishes at $r=0$. Finally, if the source distributions vanish faster than any power of r as $r\to\infty$ it can be shown that the remaining Fourier coefficients behave like

$$P_n^{(0)}\sim c_n^{\pm}r^{\pm n}\quad\text{as}\quad r\to\infty,\quad n\neq 0.$$

This solution is not valid at large distances from the jet. Hence, in order to determine the properties of the sound in the radiation field we must construct an outer expansion. To this end we introduce the outer variable

$$\tilde{r}=\epsilon r \quad (7)$$

into (2) and expand its solution for the limit $\epsilon\to0$ with $\tilde{r}$ held fixed. Then, if we again assume that both the mean velocity field of the jet and the source distribu-

tion vanish sufficiently fast as $r \to \infty$, (2) will reduce to the ordinary wave equation†

$$\tilde{\nabla}_t^2 P + (M^2 - \kappa^2) P = 0,$$

where $\tilde{\nabla}_t^2$ is the transverse Laplacian $\epsilon^{-2}\nabla_t^2$ in the outer variables. Consequently, the outer expansion is

$$P = \tilde{P}^{(0)}(\tilde{r}, \phi) + \epsilon \tilde{P}^{(1)}(\tilde{r}, \phi) + \beta(\epsilon)\tilde{P}^{(2)}(\tilde{r}, \phi) + \ldots, \quad \beta(\epsilon) = o(\epsilon), \tag{8}$$

and, at least for the first few m, the $\tilde{P}^{(m)}$ are determined by

$$\tilde{\nabla}^2 \tilde{P}^{(m)} + K^2 \tilde{P}^{(m)} = 0,$$

where we have put

$$K = (M^2 - \kappa^2)^{\frac{1}{2}}. \tag{9}$$

This equation will possess an outgoing-wave solution only if K is real, in which case the solution can be written as

$$\tilde{P}^{(m)} = \sum_{n=-\infty}^{\infty} C_n^{(m)}(k, \epsilon) H_n^{(1)}(K\tilde{r}) e^{in\phi}, \tag{10}$$

where the $H_n^{(1)}$ denote the Hankel functions.

The constants b_0, $c_n^{\pm}$ and $C_n^{(m)}$ are determined by requiring that inner and outer expansions 'match' to the proper order in some intermediate region. This can be accomplished either by using the matching principle of Van Dyke (1964, p. 64) or by introducing intermediate variables and re-expanding in the overlap domain (Cole 1968, p. 234). In either case we find that

$$\left.\begin{aligned} P^{(-1)} &= \text{constant}, \quad \tilde{P}^{(0)} = 0, \\ C_{\pm 1}^{(1)} &= \pm \tfrac{1}{2} i K \pi c_{\pm 1}^{-}, \\ C_n^{(1)} &= 0, \quad n \neq \pm 1. \end{aligned}\right\} \tag{11}$$

Hence it follows from (1) and (7)–(11) that, to lowest order in ϵ, the pressure fluctuation in the outer region is given by

$$\begin{aligned} p \sim \int_{-\infty}^{\infty}\int_{-\infty}^{\infty} \epsilon \exp\left[-i\epsilon\{\kappa(Z - Z_0(\tau)) + (\tau + \kappa Z_0(\tau))\}\right] \\ \times (e^{i\phi} C_1^{(1)} - e^{-i\phi} C_{-1}^{(1)}) H_1^{(1)}(\epsilon K r)\, dk\, d\epsilon, \end{aligned}$$

where $Z_0(\tau)$ has been added and subtracted in the exponent for future convenience. (If the source region is moving Z_0 can be thought of as the axial co-ordinate of this region at some appropriate time. If the source region is stationary no generality is lost if Z_0 is set equal to zero.)

When r is much larger than a wavelength we can replace the Hankel function $H_1^{(1)}$ in the preceding equation by its asymptotic expansion to obtain

$$\begin{aligned} p \sim \frac{r_0}{8\pi}\left(\frac{2}{i\pi r}\right)^{\frac{1}{2}} \int_{-\infty}^{\infty}\int_{-\infty}^{\infty} \frac{\exp\{-i\epsilon[\kappa(Z - Z_0) - Kr]\}}{(K\epsilon)^{\frac{1}{2}}} \epsilon \exp\left[-i\epsilon(\tau + \kappa Z_0)\right] \\ \times \mathscr{P}(k, \epsilon|\phi)\, dk\, d\epsilon, \end{aligned}$$

† At least to any order of ϵ which is of interest.

$$\mathscr{P}(k,\epsilon|\phi) \equiv \frac{1}{2\pi}\int_{-\infty}^{\infty}\int \exp\left[i\epsilon(\kappa\hat{Z}+\tau)\right]\frac{1}{[1+\kappa U(\hat{r})]^2}K \times \mathbf{f}_t.\hat{\nabla}\left[\frac{Y_1(\kappa,\hat{r})}{Y_1'(\kappa,\infty)}\cos(\phi-\hat{\phi})\right]d\hat{\mathbf{y}}\,d\tau,$$

where $\hat{r}$, $\hat{\phi}$ and $\hat{Z}$ are the cylindrical co-ordinates of the source point $\mathbf{y}$ and $\hat{\nabla}$ is the divergence operator in these variables. Then, applying the method of stationary phase to this result in the same way as in I, we find that as $R\to\infty$

$$p \sim \frac{r_0}{4\pi i R}\int_{-\infty}^{\infty} \epsilon \exp\{i\epsilon[MR-(\tau-MZ_0\cos\theta)]\}\,\mathscr{P}(-\epsilon M\cos\theta,\epsilon|\phi)\,d\epsilon, \quad (12)$$

where

$$\mathscr{P}(-\epsilon M\cos\theta,\epsilon|\phi) = \frac{M}{2\pi}\int_{-\infty}^{\infty}\int \exp\left[i\epsilon(\tau-\hat{Z}M\cos\theta)\right] \times \frac{\sin\theta}{(1-MU\cos\theta)^2}\mathbf{f}_t.\hat{\nabla}[\cos(\phi-\hat{\phi})\,J(\theta,\hat{r})]\,d\hat{\mathbf{y}}\,d\tau,$$

$$J(\theta,\hat{r}) \equiv Y_1(-M\cos\theta,\hat{r})/Y_1'(-M\cos\theta,\infty),$$

U is now a function of $\hat{r}$ and, as in I, we have introduced the polar co-ordinates

$$R \equiv \{r^2+[Z-Z_0(\tau)]^2\}^{\frac{1}{2}}, \quad \theta = \tan^{-1}[r/(Z-Z_0(\tau))].$$

Upon explicitly introducing the lateral dipole and quadrupole sources by means of equation (3) of I, integrating the quadrupole terms by parts and recognizing that Y_1 is a homogeneous solution of (4), we obtain

$$\mathscr{P} = \mathscr{P}_D + \mathscr{P}_Q, \quad (13)$$

where

$$\mathscr{P}_D = \frac{M}{2\pi}\int_{-\infty}^{\infty}\int \frac{\exp\left[i\epsilon(\tau-\hat{Z}M\cos\theta)\right]}{(1-MU\cos\theta)^2} \times \sin\theta[D_r\cos(\phi-\hat{\phi})\,J'(\theta,\hat{r})+\hat{r}^{-1}D_\phi\sin(\phi-\hat{\phi})\,J(\theta,\hat{r})]\,d\hat{\mathbf{y}}\,d\tau, \quad (14)$$

$$\mathscr{P}_Q = \frac{M}{2\pi}\int_{-\infty}^{\infty}\int \exp\left[i\epsilon(\tau-\hat{Z}M\cos\theta)\right] \times \left\{\frac{-2MU'\cos\theta}{r_0(1-MU\cos\theta)^3}\sin\theta\sin(\phi-\hat{\phi})\frac{J(\theta,\hat{r})}{\hat{r}}T_{r\phi} + \frac{\sin\theta}{r_0(1-MU\cos\theta)^2}\frac{\partial}{\partial\hat{r}}\left[\frac{1}{\hat{r}}J(\theta,\hat{r})\right][(T_{rr}-T_{\phi\phi})\cos(\phi-\hat{\phi}) - 2T_{r\phi}\sin(\phi-\hat{\phi})]\right\}d\hat{\mathbf{y}}\,d\tau, \quad (15)$$

the primes now denote differentiation with respect to the co-ordinate $\hat{r}$ and the subscripts r and ϕ denote components of the vector or tensor $\mathbf{D}$ or $\mathbf{T}$ along these directions. This is the final expression for the far-field acoustic pressure fluctuations due to the components of the dipole and quadrupole sources which were not considered in I. The formula contains the quantity J, which depends on the homogeneous solution of (4). We do not have an explicit formula for this solution for the case of an arbitrary velocity profile. But for a power-law velocity profile,

it may be expressed in terms of the hypergeometric function $F(\alpha, \beta, \gamma; t)$ by equation (B 1) of appendix B. In order to understand the significance of this result it is useful to consider the special case of point sources carried along at the local velocity of the flow.

Convected point sources

Consider a harmonic point source with dimensionless frequency ϵ_0 moving with a convection velocity U_c (which may in general be different from the local jet velocity $U(r_s)\,U_s$ at the dimensionless source radius r_s). For convenience we take the normalizing velocity U_s to be the source convection velocity U_c. In order to emphasize this choice we shall write M_c in place of $M \equiv U_s/a_0$. Then the source strengths must be of the form

$$S = \frac{1}{r_0^3}\exp(-i\epsilon_0\tau)\,\delta(\hat{Z}-\tau)\frac{\delta(\hat{r}-r_s)}{\hat{r}}\delta(\hat{\phi})\,S^{(0)}, \tag{16}$$

where the symbol S is used to designate any of the source strengths D_r, D_θ, $T_{r\phi}$, etc.

For purposes of comparison we take $Z_0(\tau)$ to be the dimensionless position of the source at the emission time $r_0(\tau/U_c - R/a_0)$ of the sound wave reaching the point $(r_0 r,\ \phi,\ r_0 Z)$ at the time $r_0\tau/U_c$. Thus

$$Z_0 = \tau - M_c R. \tag{17}$$

Then inserting (16) into (14) shows that

$$\mathscr{P}_D(-\epsilon M_c\cos\theta, \epsilon) = \frac{M_c\,\delta(\epsilon_0-\epsilon(1-M_c\cos\theta))}{r_0^3\,(1-M_j\cos\theta)^2}$$
$$\times \sin\theta[D_r^{(0)}\cos\phi\,J_c'(\theta, r_s) + r_s^{-1}D_\phi^{(0)}\sin\phi\,J_c(\theta, r_s)],$$

where $M_j \equiv U(r_s)\,M_c$ is the local jet Mach number at the radial location of the source, $M_j' \equiv M_c\,U'(r_s)$ is the Mach number gradient at the source location,

$$J_c \equiv Y_1(-M_c\cos\theta, r_s)/Y_1'(-M_c\cos\theta, \infty) \tag{18}$$

and a similar expression holds for $\mathscr{P}_Q$. Inserting these results together with (17) into (12) now shows that the pressure fluctuations at sufficiently large values of the distance $r_0 R$ between the observation point and the source emission point are given by

$$p = p_D + p_Q,$$

where

$$p_D \sim \frac{(M_c\epsilon_0/r_0)\sin\theta}{4\pi i r_0 R(1-M_c\cos\theta)^2(1-M_j\cos\theta)^2}\left\{(D_r^{(0)}\cos\phi + D_\phi^{(0)}\sin\phi)\frac{J_c(\theta, r_s)}{r_s}\right.$$
$$\left. + r_s\left[\frac{\partial}{\partial r_s}\frac{J_c(\theta, r_s)}{r_s}\right]D_r^{(0)}\cos\phi\right\}\exp[i\epsilon_0(M_c R-\tau)], \tag{19}$$

$$p_Q \sim \frac{(M_c\epsilon_0/r_0)}{4\pi i(r_0 R)\,(1-M_c\cos\theta)^2}\left\{\frac{-2M_j'\cos\theta}{r_0(1-M_j\cos\theta)^3}\sin\theta\sin\phi\frac{J_c(\theta, r_s)}{r_s}T_{r\phi}^{(0)}\right.$$
$$+\frac{\sin\theta}{r_0(1-M_j\cos\theta)^2}\frac{\partial}{\partial r_s}\left[\frac{1}{r_s}J_c(\theta, r_s)\right]\left[\left(T_{rr}^{(0)}-T_{\phi\phi}^{(0)}\right)\cos\phi - 2T_{r\phi}^{(0)}\sin\phi\right]\Bigg\}$$
$$\times\exp[i\epsilon_0(M_c R-\tau)]. \tag{20}$$

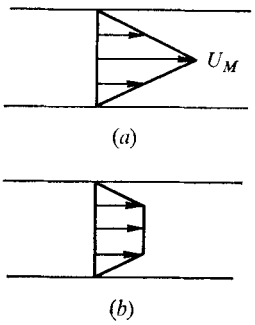

FIGURE 1. Specific jet velocity profiles. (*a*) Linear profile. (*b*) Trapezoidal profile.

The results of appendix B show that, for the power-law velocity profile (see figure 1*a*) $U = U_M(1-r^\lambda)$,

$$J_c = \frac{\mu r_s(1-M_j\cos\theta)^{-\gamma}F(\gamma,3+\gamma;\mu;r_s^\lambda M_M\cos\theta/(1-M_j\cos\theta))}{\mu F(\gamma,3+\gamma;\mu;M_M\cos\theta)+M_M\cos\theta F(1+\gamma,3+\gamma;\mu+1;M_M\cos\theta)}, \quad (21)$$

where $$\gamma \equiv \lambda^{-1}-1+(1+\lambda^{-2})^{\frac{1}{2}}, \quad \mu \equiv 2\lambda^{-1}+1,$$

$M_M = U_M M_c$ is the Mach number at the centre-line of the jet and the exponent λ of the velocity profile can be any positive number. Similar expressions can be obtained for the trapezoidal profile shown in figure 1(*b*) but we shall, for simplicity, restrict our attention to the power-law profile.

3. Approximate formulae

The complexity of this expression for J_c makes it difficult to interpret the physical content of (19) and (20). But expanding (21) about $\cos\theta = 0$ (i.e. $\theta = 90°$) shows that

$$J_c = r_s(1-\eta_0 M_j\cos\theta)+O(\cos^2\theta) \quad \text{as} \quad \theta\to\tfrac{1}{2}\pi,$$

where $$\eta_0 = (1-2\lambda^{-1}\mu^{-1}r_s^\lambda)/(1-r_s^\lambda). \quad (22)$$

Hence $$J_c = r_s(1-M_j\cos\theta)^{\eta_0}+O(\cos^2\theta) \quad \text{as} \quad \theta\to\tfrac{1}{2}\pi, \quad (23)$$

and this function will provide a fairly good fit to the true value of J_c over the entire range of θ. The approximate expression (23) is compared with the exact formula (21) for $\lambda = 1$ in figure 2.

Similarly, expanding $\partial[r_s^{-1}J_c(\theta,r_s)]/\partial r_s$ about $\cos\theta = 0$ shows that

$$\frac{\partial}{\partial r_s}\left\{\frac{1}{r_s}[J_c(\theta,r_s)]\right\} = \frac{2}{\mu}M_M r_s^{\lambda-1}\cos\theta(1-\eta_1 M_j\cos\theta)+O(\cos^2\theta) \quad \text{as} \quad \theta\to\tfrac{1}{2}\pi, \quad (24)$$

where $$\eta_1 = -r_s^\lambda/(\mu+1)(1-r_s^\lambda). \quad (25)$$

Hence

$$\frac{\partial}{\partial r_s}\left[\frac{1}{r_s}J_c(\theta,r_s)\right] = -\frac{2}{\lambda\mu}M_j'\cos\theta(1-M_j\cos\theta)^{\eta_1}+O(\cos^2\theta) \quad \text{as} \quad \theta\to\tfrac{1}{2}\pi, \quad (26)$$

and we again obtain a fair approximation to the true value of $\partial(r_s^{-1}J_c)/\partial r_s$ for the whole range of θ. The approximate expression (26) is compared with the exact result for $\lambda = 1$ [obtained by differentiating (21)] in figure 3.

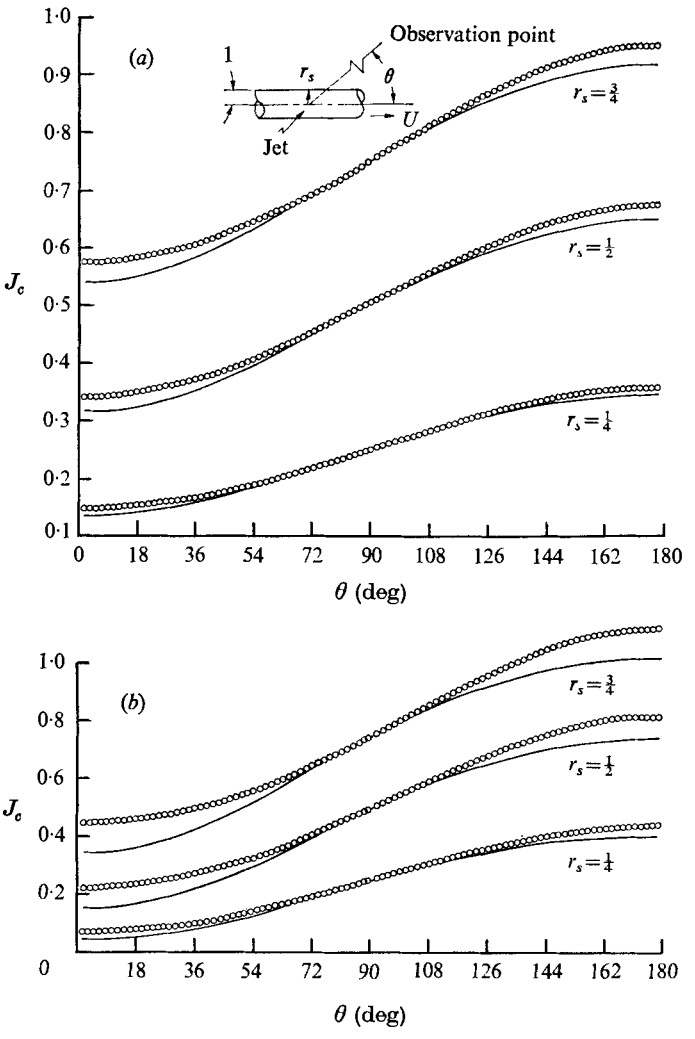

FIGURE 2. Comparison of exact and approximate formulae for J_c for $\lambda = 1$. ——, exact equation (21); ○, approximate equation (23). (*a*) $M_M = 0{\cdot}5$. (*b*) $M_M = 0.9$.

Upon inserting the approximate formulae (23) and (26) into (19) and (20) we get

$$p_D \sim \frac{(M_c\epsilon_0/r_0)\sin\theta}{4\pi i(r_0R)(1-M_c\cos\theta)^2}\left[\frac{D_r^{(0)}\cos\phi + D_\phi^{(0)}\sin\phi}{(1-M_j\cos\theta)^{2-\eta_0}} - \frac{2r_sM_j'\cos\theta\cos\phi\, D_r^{(0)}}{\lambda\mu(1-M_j\cos\theta)^{2-\eta_1}}\right]\exp\left[i\epsilon_0(M_cR-\tau)\right], \tag{27}$$

$$p_Q \sim \frac{-(M_c\epsilon_0/r_0)M_j'\cos\theta\sin\theta}{4\pi i(r_0R)(1-M_c\cos\theta)^2 r_0}\left[\frac{2\sin\phi\, T_{r\phi}^{(0)}}{(1-M_j\cos\theta)^{3-\eta_0}} + \frac{2[(T_{rr}^{(0)}-T_{\phi\phi}^{(0)})\cos\phi - 2rT_{r\phi}^{(0)}\sin\phi]}{\lambda\mu(1-M_j\cos\theta)^{2-\eta_1}}\right]\exp\left[i\epsilon_0(M_cR-\tau)\right]. \tag{28}$$

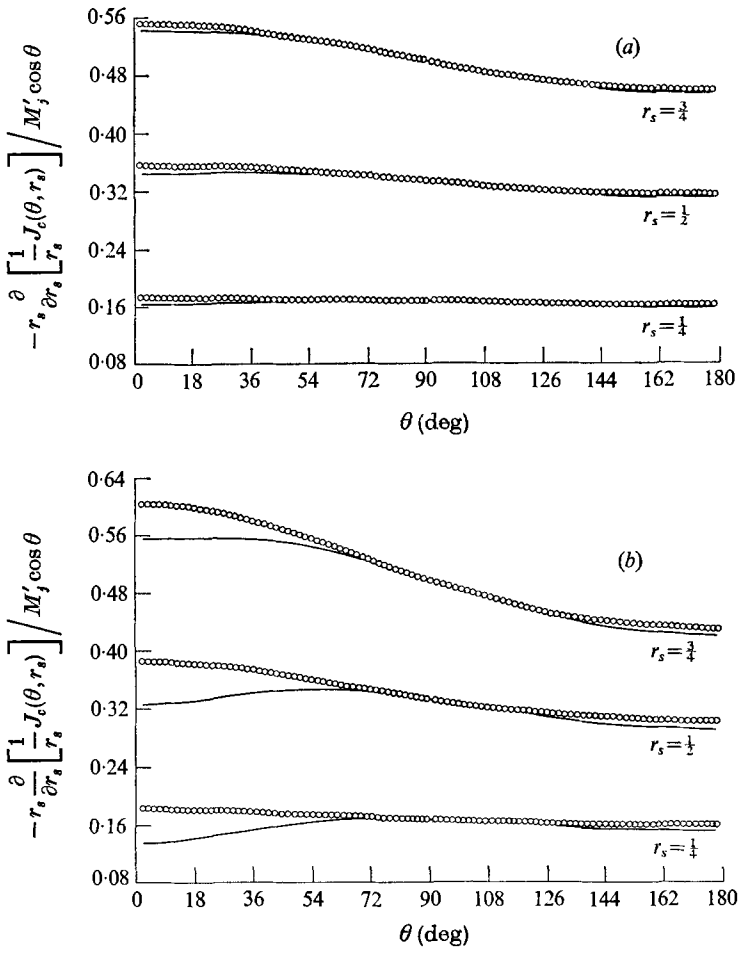

FIGURE 3. Comparison of exact and approximate formulae for the derivative of J_c for $\lambda = 1$. ——, exact, from equation (21); ○, approximate equation (26). (*a*) $M_M = 0{\cdot}5$. (*b*) $M_M = 0{\cdot}9$.

4. Discussion of results

As was done in I, it is instructive to compare these results with the corresponding formulae for point sources moving through a medium at rest. (For simplicity we restrict our attention to the case where $M_j = M_c = M$. Nevertheless, it should be kept in mind that part of the Doppler factor is associated with the source convection effects, which will be present even when the sources are moving through a stationary medium.) The results therefore show how the mean-flow interaction effects modify the acoustic radiation patterns that arise from freely convecting source models. The predominant difference in the dipole source comes from the change in the exponent n of the Doppler factor $(1-M\cos\theta)^{-n}$, while for the quadrupole there is in addition an augmentation of the acoustic efficiency of the source to the level of the dipole. These effects were also observed for the components of the sources considered in I. In the

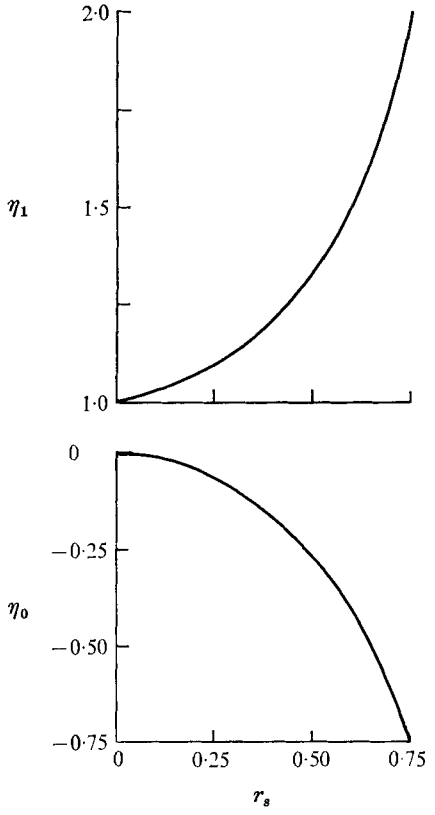

FIGURE 4. Variation of Doppler-factor exponents with source position for $\lambda = 1$.

present case there is also a relatively small modification of the directivity pattern due to the deviation of the approximate values of J_c and J_c' from the values predicted by the exact equations. More important, however, the modification of the exponent of the Doppler factors is different from that for the sources considered in I and the nature of this modification now depends on both the position of the sources within the jet and the shape of the velocity profile (owing to the dependence of η_0 and η_1 on r_s and λ). These functions [which are given by (22) and (25)] are plotted for $\lambda = 1$ in figure 4. It can be seen from this figure that η_0 varies roughly between one and two. Hence the first terms in (27) and (28) have Doppler factors whose exponents are always smaller than those of the corresponding sources in I, and in fact when the sources are located near the edge of the jet, their Doppler factors approach those of sources moving through a medium at rest. The figure also shows that η_1 has a value near zero for small r_s and becomes increasingly negative as $r_s \to 1$. Hence the second groups of terms in (27) and (28) represent sources which, when near the jet axis, have Doppler-factor exponents that are less than or equal to those of the sources in I. (The exponents for the dipole sources are equal while those for the quadrupole are not.) When these sources are moved towards the outside of the jet, the exponents increase. However, as can be seen from figure 4, most of this increase occurs when the sources are very near the

edge of the jet (and hence are moving with very low velocities). Over most of the range of source positions the exponent of the quadrupole source is less than 5 (which is the exponent found in I) and that of the dipole source is less than 4 (which is greater by one than the exponent found in I). The results for other velocity profiles are similar. Notice that the magnitude of η_1 increases with increasing λ while η_0 approaches a constant as $\lambda \to 0$.

Another remarkable difference between the present quadrupole sources and those moving through an undisturbed medium is due to the factor $\sin\theta\cos\theta$ multiplying (28). Thus the sources in this equation all represent quadrupoles whose axes are transverse to the Z direction. In the absence of a mean flow such quadrupoles exhibit directivity patterns which vary like $\sin^2\theta$ and hence vanish only on the jet axis. The radiation field from the present sources vanishes both on the jet axis and at 90° to this axis. All the quadrupole sources as well as the part of the dipole source due to the second term in (27) behave in this manner. It should be noted that, like the quadrupole sources, the latter term is proportional to the local Mach number gradient.

Appendix A

Since (4) has two linearly independent homogeneous solutions, say Y_1 and Y_2, which behave like

$$Y_1 \sim \text{constant} \times r, \quad Y_2 \sim \text{constant} \times r^{-1}$$

at the regular singular point $r = 0$, its solution which remains bounded at $r = 0$ is given by

$$P_{\pm 1}^{(0)} = A_\pm Y_1(r) - Y_1(r)\int_\infty^r \frac{Y_2(s)\,F_\pm(s)}{W(s)}\,ds + Y_2(r)\int_0^r \frac{Y_1(s)\,F_\pm(s)}{W(s)}\,ds, \tag{A 1}$$

where we have put

$$F_\pm(r) \equiv \frac{(1+\kappa U)^2 r_0}{(2\pi)^3}\int_0^{2\pi}\int_{-\infty}^{\infty}\int_{-\infty}^{\infty} \exp\left[i\epsilon(\kappa Z+\tau) \mp i\phi\right] \nabla\cdot\left[\frac{\mathbf{f}_t}{(1+\kappa U)^2}\right] dZ\,d\phi\,d\tau \tag{A 2}$$

and

$$W(r) \equiv Y_1(r)\,Y_2'(r) - Y_2(r)\,Y_1'(r) = \text{constant} \times (1+\kappa U)^2/r \tag{A 3}$$

denotes the Wronskian of Y_1 and Y_2.

If $U \to 0$ sufficiently rapidly as $r \to \infty$, Y_1 and Y_2 must behave like

$$Y_1 \sim a_{11}/r + a_{12} r, \quad Y_2 \sim a_{21}/r + a_{22} r \quad \text{as} \quad r \to \infty \tag{A 4}$$

to within terms of negligibly small order. Hence $P_{\pm 1}^{(0)}$ will remain bounded at infinity only if we put

$$A_\pm = -\frac{a_{22}}{a_{12}}\int_0^\infty \frac{Y_1(r)\,F_\pm(r)}{W(r)}\,dr.$$

Then, since it follows from (A 4) that $W(r) \sim 2(a_{11}a_{22} - a_{21}a_{12})/r$ as $r \to \infty$ and $Y_1'(\infty) = a_{12}$, the solution (A 1) which remains bounded at infinity behaves like

$$P_{\pm 1}^{(0)} \sim \frac{-1}{2rY_1'(\infty)}\int_0^\infty \frac{Y_1(r)\,F_\pm(r)}{(1+\kappa U)^2}\,r\,dr \quad \text{as} \quad r \to \infty. \tag{A 5}$$

Appendix B

In the special case where the velocity profile is a function of the form

$$U = \begin{cases} U_M(1-r^\lambda), & 0 < r < 1, \\ 0, & r > 1, \end{cases}$$

where the exponent λ is an arbitrary positive constant, Y_1, the homogeneous solution of (4) which remains bounded at $r = 0$, can be expressed in terms of the hypergeometric function $F(a, b; c; z)$ as

$$\begin{aligned} Y_1 &= \xi^{1/\lambda} F(\gamma, \mu-\gamma-3; \mu; \xi) \\ &= \frac{\xi^{1/\lambda}}{(1-\xi)^\gamma} F\left(\gamma, 3+\gamma; \mu; \frac{\xi}{\xi-1}\right), \end{aligned} \tag{B 1}$$

where $\xi \equiv \kappa U_M r^\lambda/(1+\kappa U_M)$, $\gamma \equiv \lambda^{-1} - 1 + (1+\lambda^{-2})^{\frac{1}{2}}$, $\mu \equiv 2\lambda^{-1}+1$.

The first expression holds for ξ in the range $0 < \xi < 1$ while the second holds in the range $\xi < \frac{1}{2}$. For our purposes the latter form is preferable since only those values of κU_M whose magnitude is less than unity can influence the far-field pressure and, for these values, the second expression will have a convergent power-series expansion for all r in the range $0 < r < 1$.

For $r > 0$ the solution is

$$Y_1 = a/r + br, \quad r > 1.$$

But if Y_1 and dY_1/dr are to be continuous at $r = 1$ we must require that

$$\begin{aligned} b = (1+\kappa U_M)^\gamma \left(\frac{\kappa U_M}{1+\kappa U_M}\right)^{1/\lambda} &[F(\gamma, 3+\gamma; \mu; -\kappa U_M) \\ &- \mu^{-1}\kappa U_M F(1+\gamma, 3+\gamma; 1+\mu; -\kappa U_M)]. \end{aligned}$$

Hence

$$\frac{Y_1'(\kappa, r)}{Y_1'(\infty)} = \frac{\mu(1+\kappa U)^{-\gamma} r F(\gamma, 3+\gamma; \mu; \xi/(\xi-1))}{\mu F(\gamma, 3+\gamma; \mu; -\kappa U_M) - \kappa U_M F(1+\gamma, 3+\gamma; 1+\mu; -\kappa U_M)}.$$

REFERENCES

COLE, J. D. 1968 *Perturbation Methods in Applied Mathematics.* Blaisdell.

GOLDSTEIN, M. 1975 The low frequency sound from multipole sources in axisymmetric shear flows, with applications to jet noise. *J. Fluid Mech.* **70**, 595.

VAN DYKE, M. 1964 *Perturbation Methods in Fluid Mechanics.* Academic.